Research article

Influence of interaction between organic cation and inorganic unit in bi-based hybrid perovskites for photoelectronic properties

Liuyuan Han [a,*], Qian Wu [b], Longfei Lei [c], Jinghang Chen [c], Ni Xue [c]

[a] Qingdao Institute of Bioenergy and Bioprocess Technology, Chinese Academy of Sciences, Shandong 266101, China
[b] School of Physics, Shandong University, Shandong 250100, China
[c] State Key Laboratory of Crystal Materials, Shandong University, Shandong 250100, China

ARTICLE INFO

ABSTRACT

With the increase of the passion on lead-free perovskites, more and more endeavor focused on halobismuthates. Here, we have introduced the *p*-iodoaniline and *p*-phenylenediamine into Bi-based hybrid materials, and two photoactive iodobismuthate named *p*-phenylenediamine iodobismuthate (PDABI) and *p*-iodoaniline iodobismuthate (PIDBI) were prepared. Their single structures, band gaps, thermostability and other properties were explored. The structure results revealed that they all have 1D BiI_4^- anion chains with edge-shared BiI_6 octahedron. The DFT result revealed that PIDBI had an inherent interaction between the I substituent in *p*-iodoaniline cation and the Bi atom in inorganic BiI_4 anion chains. The photodetector assembled by PDABI and PIDBI revealed that the interaction provided by symmetric *p*-phenylenediamine has a positive effect on PIDBI's optoelectronic properties compared to the role of asymmetric *p*-iodoaniline in PDABI.

1. Introduction

Metal-organic-inorganic hybrid materials have been studied as a promising light absorbing material in recent years. Among those hybrids, bismuth-based materials have many advantages and become a research hotspot recently [1]. However, there are also some questions on halobismuthate materials. For example, the reason why Bi-based materials have low photoelectric efficiency is still not clearly explanted [2]. To answer this question, some researchers embarked on exploring the structure of anions or cations to study the influence of anions with different configurations on their photoelectric properties, such as single or double chains [3], zigzag chains [4], ring-contained chains [5], spiral chains [6], etc [7]. Hamdeh revealed that in hybrid materials, the cation size mismatch had no discernible impact on the band gap. Other preliminary conclusions also have been proposed, such as they proposed to induce an inner chemical pressure by designing cation alloys with associated size mismatch [8]. In addition, the hybrid materials composed of Bi^{3+} have lone $6s^2$ electron pairs, which will be beneficial for the formation of one-dimensional (1D) or two-dimensional (2D) materials [9, 10]. More and more studies start proposed that the construction of charge transfer dimension of hybrid materials is beneficial to improve its

photoelectric properties and other properties [11]. Many literatures have achieved good results by building electron transport connections in Bi-based hybrid materials to improve their photoelectric properties, such as I_2 molecules [12], I^{3-} ions [13], HI molecules [14], water molecules [15], even solvent molecules [16] and so on [17].

The resent studies on the construction of intermolecular connections in 1D hybrid materials were reported that the BiI_4^- ion often forms 1D chains with strong quantum confinement and dielectric confinement [18]. Researchers tried using symmetric divalent cations to further improve the interaction between cationic and anions, including strong or weak interactions [19]. They also proposed that interactions can reduce the negative effects of confinement and dielectric effect by increasing the dimensionality of bismuth-based perovskites, to improve target photoelectric properties.

However, we all know a fact that even a very small change in study material's substructure also resulted in a series of continuous changes in its structure and properties. Multiple changes in structure make it more difficult for researchers in explanting the relationship between structure and property. The weak interaction between cation and cation is often underestimated [20]. Therefore, by designing a pair of compounds that as similar as possible in structure sufficiently, then investigating their

---

* Corresponding author.
  E-mail address: hanly@qibebt.ac.cn (L. Han).

Table 1. Experimental crystallographic parameters from single crystal diffraction of PDABI and PIDBI.

	PDABI	PIDBI
Chemical formula	$C_6H_9N_2BiI_4$	$C_{12}H_{14}N_2Bi_2I_{10}$
Formula wt (g/mol)	825.73	1873.21
Crystal system, space group	Orthorhombic, *Pbca*	Triclinic, $P\bar{1}$
Temperature (K)	296	296
a, b, c (Å)	15.5723 (5), 7.7862 (2), 24.4709 (7)	10.9144 (4), 11.3609 (5), 13.6647 (6)
α, β, γ (°)	90.000 (0), 90.000 (0), 90.000 (0)	76.455 (1), 74.072 (2), 85.582 (1)
V (Å³)	2967.07 (15)	1583.87 (12)
Z	8	2
Radiation type	Mo *Kα*	Mo *Kα*
μ (mm⁻¹)	20.18	20.85
Crystal size (mm)	$0.16 \times 0.16 \times 0.15$	$0.18 \times 0.18 \times 0.16$
No. of measured, independent and observed $[I > 2\sigma(I)]$ reflections	20247, 3415, 3075	14394, 7175, 6444
R_{int}	0.082	0.051
$(\sin \theta/\lambda)_{max}$ (Å⁻¹)	0.651	0.649
$R\ [F^2 > 2\sigma(F^2)], wR\ (F^2), S$	0.055, 0.151, 1.10	0.053, 0.153, 1.03
No. of reflections	3415	7175
No. of parameters	120	237
$\Delta\rangle_{max}, \Delta\rangle_{min}$ (e Å⁻³)	3.93, −3.35	5.23, −4.24

similarities and differences in structure and property more effectively, same to evaluate the influence of a single factor on target properties.

Based on the above ideas, we have introduced the *p*-iodoaniline and *p*-phenylenediamine into Bi-based hybrid materials, and two photoactive iodobismuthate named *p*-phenylenediamine iodobismuthate (PDABI) and *p*-iodoaniline iodobismuthate (PIDBI) were prepared. Their crystal structures, band gaps, thermostability and other properties were explored. The single-XRD results revealed that they all have 1D BiI_4^- anion chains with edge-shared BiI_6 octahedron. The DFT revealed PIDBI has a weak interaction between the I substituent in cation and Bi atom in inorganic chain. The photodetector fabricated by PDABI and PIDBI revealed that the interaction provided by symmetric *p*-phenylenediamine has a positive effect on PIDBI's optoelectronic properties compared to the role of asymmetric *p*-iodoaniline in PDABI.

2. Experimental section

2.1. Materials

Synthesis of PDABI. Solution A: 2.00 g Bi_2O_3 (99%) was dissolved in 7.10 g HI (55%) with stirring, subsequently 30 mL methanol was dropped in. Solution B: 1.38 g *p*-phenylenediamine (AR) was dissolved in 5 mL methanol with stirring, subsequently 2.89 g HI (55%) was added. Then solution B was added into solution A drop by drop. The mixture was stirring for a while and then put into a tube for a few days at room temperature, red brown crystals were growth.

Synthesis of PIDBI. The procedure was similar to that of PDABI, using *p*-iodoaniline (2.76 g) as a reagent.

Synthesis of PDABI film. 1.65 g PDABI crystals dissolved in 10 mL ethanol to form a solution, then dropped 50 μL solution on to the Au interdigital electrode. After vacuum drying, the film was prepared.

Synthesis of PIDBI film. The procedure was similar to that of PDABI film, using PIDBI (1.87 g) as a reagent.

2.2. Characterization of samples

X-ray diffraction studies (XRD) were carried out on powder samples with Bruker AXS D8 using Cu Kα radiation (λ = 1.5418 Å) at 0.02°/step. The PDABI and PIDBI single crystal data were carried out on Bruker SAINT diffractometer (Mo Kα radiation, λ = 0.71073 Å) with Bruker APEX-II detector at 296 K. Their thermal stability data was carried out on Mettler Toledo TGA/DSC STARe with heating rate 0.5°C/min in N_2 flow. Their UV-Vis diffuse reflectance spectra were carried out on Shimadzu UV 2550. The Raman data were carried out on LabRAM HR Evolution with a 733 nm laser. The photoluminescence (PL) spectrums were carried out on Fluoro Max-4 (Japan). Their FTIR data were carried out on NEXUS 670.

Their crystallographic data have been deposed in the Cambridge Crystallographic Data Centre (CCDC) with the deposition number 2071544 for PDABI and 2071543 for PIDBI. More detail crystal data was displayed in supporting information.

2.3. Electronic band structure calculation

As described in our early reports [21], the Vienna Ab-initio simulation package was used for first-principle density functional theory in all calculations [22]. The projector augmented wave method was used for
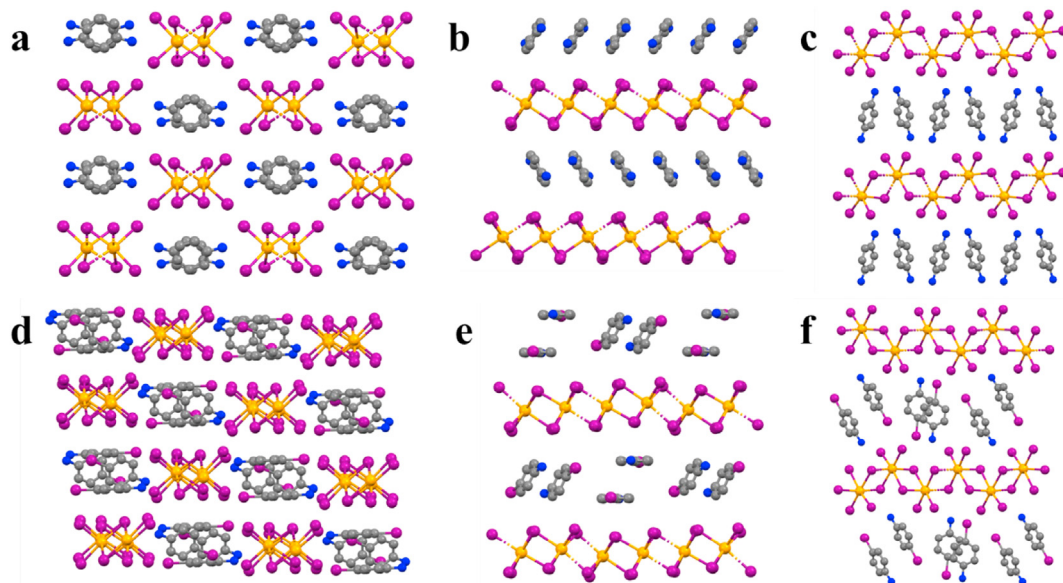

Figure 1. Crystallographic packing diagrams of PDABI (a,b,c) and PIDBI (d,e,f) viewed along different unit cell directions: a (010), b (100), c (001), d (10–1), e (111), f (1–11). C: grey; N: blue; Bi: orange; I: deep violet. Hydrogen atoms are hidden for clarity.
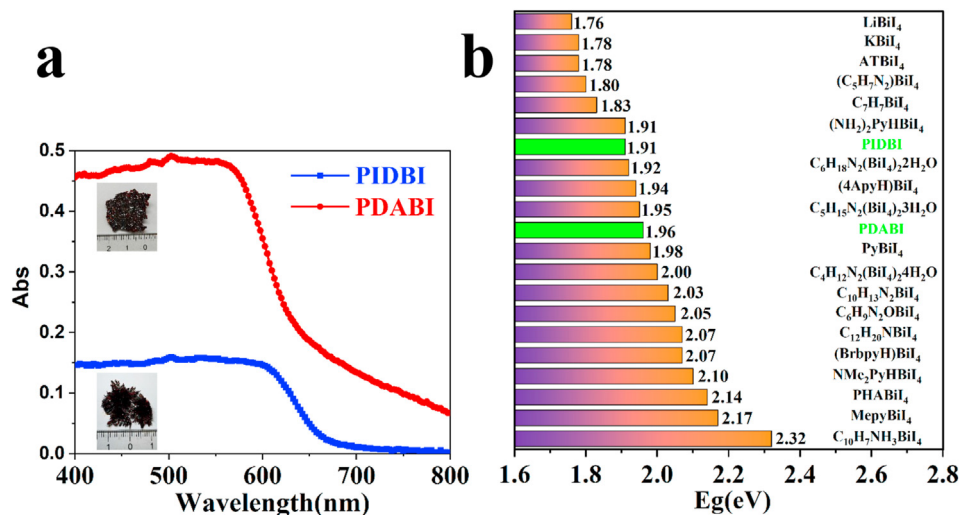
Figure 2. (a) The DRS of PDABI and PIDBI. Inset: the photograph of the crystal. (b) Band-gap energies of some iodobismuthates with BiI_4^- anion.
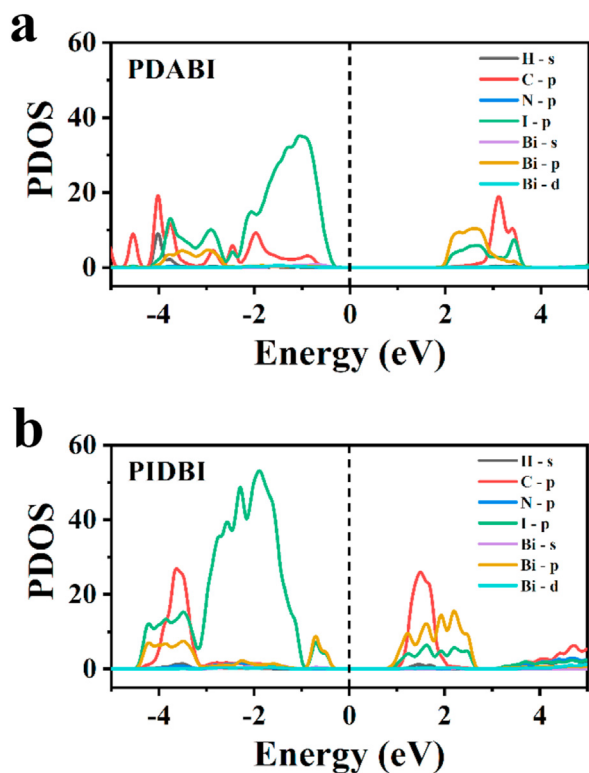

Figure 3. The DOS of PDABI and PIDBI.

ion-electron interactions [23, 24]. The generalized gradient approximation in the form of Perdew-Burke-Ernzerhof functional was used for exchange-correlation interactions [25]. The Monkhorst-Pack grid of 3 × 3×3 and 2 × 3×1 was used for Brillouin zone integration for PDABI and PIDBI, respectively. The cutoff energy, convergence criteria for energy and force was set at 500 eV, 10^{-5} eV and 0.01 eV A^{-1}, respectively.

2.4. Photoelectric measurement

The diagrammatic drawing of Au interdigital electrode was adopted as substrate (Figure S14). The Hg lamp was set at 254 nm with 500 μW/ cm^2. The effective irradiation area of the devices was 0.63 cm^2. The

photocurrent and I–V curves were measured by Keithley 2400 semiconductor characterization system.

3. Results and discussion

Since PDABI and PIDBI have never been reported before, their structures were first analyzed by single crystal X-ray diffraction in 296 K. Their experimental crystallographic parameters are shown in Table 1 and Tables S1–S8, from which can be seen that the molecular formula of PDABI is $(H_2N–C_6H_4–NH_3)BiI_4$ and that of PIDBI is $(I–C_6H_4–NH_3)_2(BiI_4)_2$. The space group of PDABI is *Pbca*, differ from $P\bar{1}$ of PIDBI, and their unit cell packing was shown in Figure S1, which revealed a high degree of symmetry in former. Additionally, their experimental X-ray diffraction patterns are good agreement with the simulated as shown in Figure S2, this result confirmed that we have resolved their single structures successfully, and further proofed the powder and the single crystal has same structure.

To compare their crystal structures more clearly, the crystallographic packing diagrams of PDABI and PIDBI viewed along different unit cell directions are shown in Figure 1, from which can be seen that their BiI_4^- anions all adopted the infinite one-dimensional (1D) chain that has been reported, such as $(C_5H_7N_2)BiI_4$ [4ApyH]BiI_4, $(C_5H_6N)BiI_4$ [26, 27, 28]. The 1D cation chains are vertical to [0, 1, 0] plane in PDABI (Figure 1a) and [−1, 0, 1] plane in PIDBI (Figure 1d), which all composed of edge-share BiI_6 octahedrons. The well-aligned 1D BiI_4^- anions were sandwiched by organic cation layers, which are parallel to other chain to form a quantum-well structure (Figure 1b, c, d, e).

It is worth noting that the $[BiI_4]_\infty$ anion chain in PDABI is similar to PIDBI at first sight, however, they are different in detail. For example, the length of the Bi–Bi bond in PDABI is 4.518 Å, which is tiny longer than the average value in PIDBI (4.499 Å). Additionally, the angle of I–Bi–I and the length of Bi–I bonds in PDABI all differ from PIDBI (Figure S3). Further analysis of their structures revealed another big difference in their cation configurations as shown in Figure S4. The *p*-iodoanilinium cation in PIDBA and p-phenylenediammonium cation in PDABI were shown in Figure S5, which displayed their big difference in benzene ring subgroup. Because the $NH_3\cdots I$ hydrogen bonds play a central role in the interactions between the organic cations and the inorganic chain framework, so the distance of $NH_3\cdots I$ interaction was further discussed. Its value was 3.601 Å in PDABI, also differ from that in PIDBI (3.629 and 3.548 Å) (Figure S4). This result revealed anther difference in their structures. Above all, even though they have a similar 1D quantum wire, the BiI_6 octahedron in PIDBI is slightly distorted compared to that in
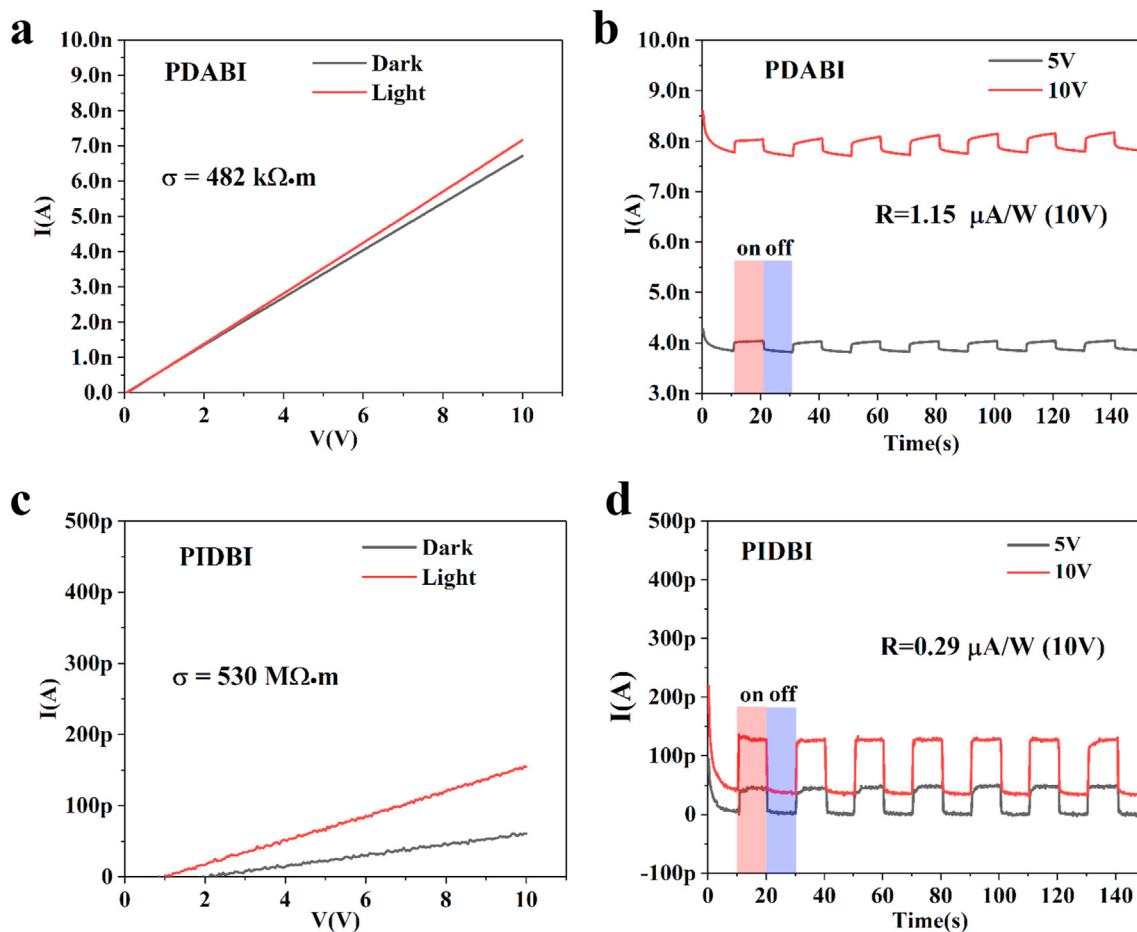
Figure 4. The I–V curves of PDABI (a) and PIDBI (c), the photocurrent of PDABI (b) and PIDBI (d).

PDABI, which will make a big difference in their physical and chemical properties.

The optical gaps of PIDBI and PDABI were determined by UV-vis diffuse reflectance spectroscopy (DRS) measurements. The photographs of their crystals were inset in Figure 2. As can be seen that they are all dark red crystal. From DRC absorption diagram, PDABI absorption edge is around 650 nm with a band gap 1.96 eV by Tauc fitting [29] (Figure S6), and 1.91 eV for PIDBI. Such close band gaps indicate that their anion structures have a similar 1D BiI_4 anion, but not exactly alike. It is well known that in halobismuthate materials, the band gap is strongly dependent on the inter-octahedra bridging angle (Bi–I–Bi angle) of the inorganic subsystem and on the octahedral distortion. As shown in Figure S3, the inter-octahedra bridging angle (Bi–I–Bi angle) and Bi–I bond distance in PDABI similar to PIDBI, but there was still tiny differ in their octahedra distortion that revealed by band gap value. Other band gaps of Bi-based material with BiI_4^- anions was shown in Figure 2b and Table S9, from which can been see that most of the Bi-based hybrid perovskites display wide band gaps of $E_g > 1.7$ eV and the compounds in this work have a typical band gap. The difference between their band gaps may result from the distorted of their BiI_4^- anions.

The Raman, PL, FTIR and thermogravimetric results are shown in Figures S7, S8, S9, S10, S11, S12. In Raman curve, peaks observed below $\sim$110 cm^{-1} corresponds to Bi–I bending modes, whereas the peaks at 120.6 and 141.6 cm^{-1} in PDABI correspond to terminal Bi–I asymmetric and symmetric stretching modes in BiI_4^- units, respectively [30]. But in PIDBI, the peaks of terminal Bi–I asymmetric and symmetric stretching mode were at 115.1 and 133.6 cm^{-1}, respectively (Figure S7). The Raman result revealed the slight difference between PDABI and PIDBI in Bi–I bending modes, which consistent with their Eg result. Resemble to

their Raman spectra, the PL peak of PDABI is 616 nm, and 649 nm for PIDBI, which revealed the existence of indirect and direct band gaps in materials (Figure S8) [31]. Similar with $(C_6H_5NH_3)BiI_4$, our crystals also has a lower PL peak than band-gap, suggesting radiative recombination involving sub-band-gap states [32]. The FTIR data revealed that the bending vibrations of N–H in a range of 3200–3500 cm^{-1} in PDABI is more complex than that in PIABI, because there are more types of N–H bonds in PDABI than in PIDBI (Figures S9, S10). Their FTIR results also give a view to compare their difference in structure, revealed the existence of $NH_3\cdots I$ hydrogen bonds. Thermogravimetric data shows that the thermal stability of PDABI is as high as 278 °C, and PIDBI's first mass-loss temperature is 176 °C (Figures S11, S12). However, their thermostability temperature all surpass 150 °C, which is consistent with the good thermal stability of Bi-based hybrid materials [33].

To further analyze the differences between PDABI and PIDBI, their valence band structures and densities of states were calculated by density functional theory (DFT) (Figures 3, S13). For PDABI, its valence band structure has a classical type that most bismuth hybrid materials have, whereas the valence band structure shows a direct band gap with an energy value of 2.05 eV at the Γ point. This is slightly higher than the experimental value of 1.96 eV, which is due to the omission of orbital spin effects in the calculation [34]. However, for PIDBI, its calculated band gap value is 1.32 eV, which is significantly smaller than the experimental value of 1.91 eV. The calculated results indicate that PIDBI has a smaller band gap, which is consistent with the experimental results. It is worth noting that in the PIDBI theoretical calculation, a new orbit composed of Bi-5p and I-5p is observed. The existence of this abnormal orbital provided clear evidence that the I atom in the cation has weak interaction with Bi atom, which differ from that of Bi–I bond in BiI_4
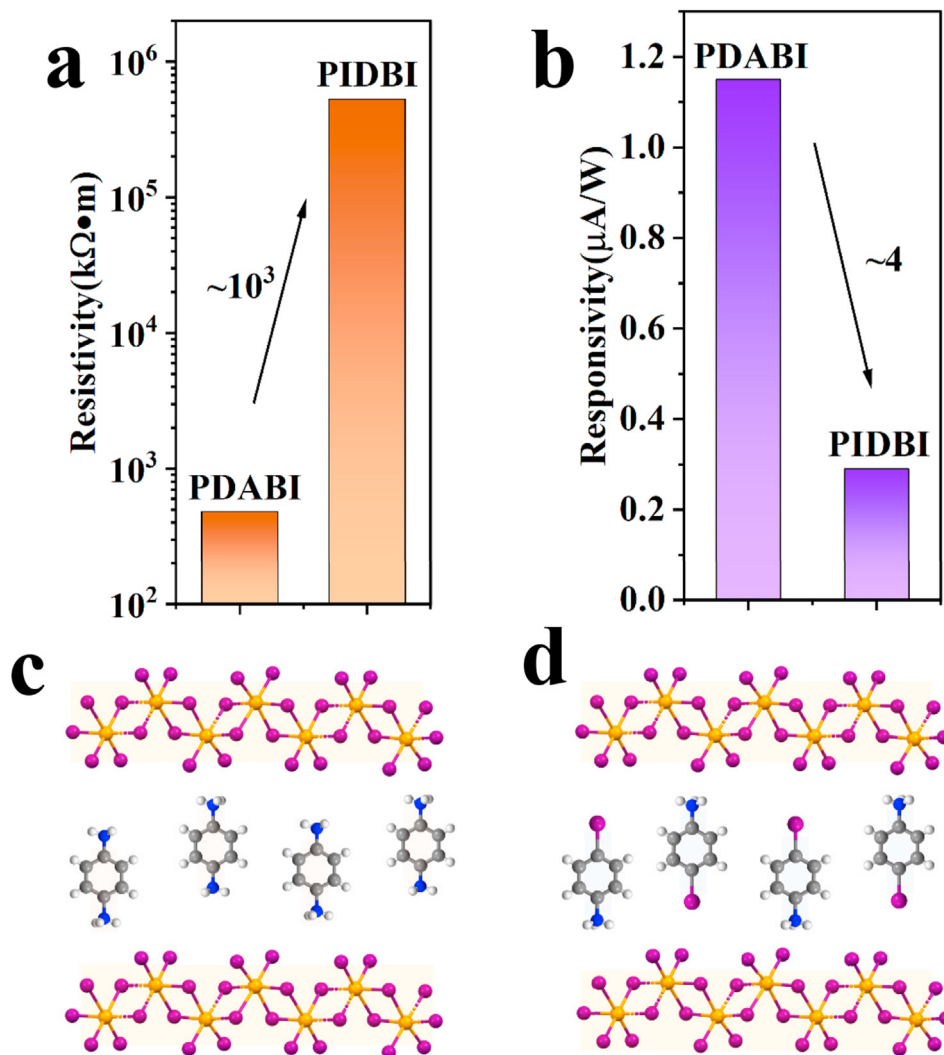
Figure 5. The comparison of resistivity (a) and responsivity (b) of PDABI and PIDBI, the electron transportation schematic diagram of PDABI (c) and PIDBI (d).

chain. This interaction may give an unpredictable effect on the electronic communication between the organic clusters and inorganic chains, thus further affecting their electronic properties.

PDABI was dissolved in methanol and then its thin films were prepared on a gold cross finger electrode (Figure S14) using a vacuum assisted evaporation solvent method [32], and similar process was done with PIDBI. To investigated their photodetector devices response to ultraviolet light as photoactive substances, a Keithey 2400 semiconductor characterization system equipped with a 254 nm UV lamp (500 $\mu W/cm^2$) was employed. The photoconductivity measurements of them were carried out and shown in Figure 4a and 4c. As can be seen from their I–V curve, they all present photoelectric response. The photocurrent of PDABI and PIDBI under different bias voltage was shown in Figure 4b and 4d, from which can be seen that the photodevices have repeatable responsivity. Those results indicate they are all photoactive materials.

Calculated from the I–V curve, the electrical resistivity of PDABI is determined to be 482 kΩ m, but it is as high as 530 MΩ m for PIDBI, with three orders of magnitude (Figure 5a). However, the responsivity of PDABI was 1.15 $\mu W/A$, about 4 times than that of PIDBI (0.29 $\mu W/A$) in Figure 5b. The results indicate that the PIDBI has low photocurrent and worse photoresponsivity than PDABI. So, the PDABI is superior to PIDBI on photoelectronic properties. Thus, it is concluded that the interactions between organic cations and inorganic chains provided by *p*-

iodoanilinium had a negative effect on the photoelectric properties in PIDBI compared to *p*-phenylenediammonium in PDABI. Otherwise, if the 1D chain is responsible for the main electron transportation (Figure 5c, 5d, background color is pale yellow), the *p*-phenylenediammonium (background color is light pink) is inclined to provide electron because the amido in benzene ring fourth site has lone pair electrons. In contrast, the iodic substituent in *p*-iodoanilinium (background color is light blue) is inclined to trap electron because the I-substituent has uncompleted 5*p* orbit, so it is reasonable that the PIDBI has high resistivity and poor optoelectronic properties. Those results will give a rule to design the Bi-based hybrid photoactive materials.

4. Conclusions

In summary, we have prepared two photoactive iodobismuthate named PDABI and PIDBI, and their single structures, band gaps and other properties were explored. They all have 1D BiI_4 anion chains with edge-shared BiI_6 octahedron. The DFT reveal there was an interaction between the I substituent in the cation and the Bi atom in the inorganic chains. The photoelectronic results revealed that the interaction provided by asymmetric *p*-iodoaniline in PDABI has a negative effect on its optoelectronic properties compared to the role of symmetric *p*-phenylenediamine. This conclusion will give a rule to design other Bi-based light absorbers.

Declarations

Author contribution statement

Liuyuan Han: Conceived and designed the experiments; Performed the experiments; Analyzed and interpreted the data; Contributed reagents, materials, analysis tools or data; Wrote the paper.

Qian Wu, Longfei Lei, Jinghang Chen, Ni Xue: Performed the experiments.

Funding statement

Data availability statement

Data included in article/supplementary material/referenced in article.

Declaration of interests statement

The authors declare no competing interests.

Additional information

Supplementary content related to this article has been published online at https://doi.org/10.1016/j.heliyon.2022.e12528.

References

[1] L. Liang, P. Gao, Lead-free hybrid perovskite absorbers for viable application: can we eat the cake and have it too? Adv. Sci. 5 (2018), 1700331.

[2] C. Wu, Q. Zhang, G. Liu, Z. Zhang, D. Wang, B. Qu, Z. Chen, L. Xiao, From Pb to Bi: a promising family of Pb-free optoelectronic materials and devices, Adv. En. Mat. 10 (2019), 1902496.

[3] S. Pandey, T. Chattopadhyay, S. Dev, Y. Patil, C.L. Carpenter-Warren, C. Sinha, Influence of cations on optical properties of iodobismuthates, Polyhedron 179 (2020), 114335.

[4] A. Gągor, M. Węcławik, B. Bondzior, R. Jakubas, Periodic and incommensurately modulated phases in a (2-methylimidazolium) tetraiodobismuthate (iii) thermochromic organic–inorganic hybrid, CrystEngComm 17 (2015) 3286–3296.

[5] A.J. Dennington, M.T. Weller, Synthesis, structure and optoelectronic properties of hybrid iodobismuthate & iodoantimonate semiconducting materials, Dalton Trans 47 (2018) 3469–3484.

[6] S. Pandey, A.P. Andrews, A. Venugopal, Manifestation of helicity in one-dimensional iodobismuthate, Dalton Trans 45 (2016) 8705–8707.

[7] W. Ning, F. Gao, Structural and functional diversity in lead-free halide perovskite materials, Adv. Mater. 31 (2019) e1900326.

[8] U.H. Hamdeh, B.J. Ryan, R.D. Nelson, M. Zembrzuski, J. Slobidsky, K.J. Prince, I. Cleveland, A. Vela-Ramirez, A.C. Hillier, M.G. Panthani, Solution-processed bismuth halide perovskite thin films: influence of deposition conditions and A-site alloying on morphology and optical properties, J. Phys. Chem. Lett. 10 (2019) 3134–3139.

[9] X. Huang, S. Huang, P. Biswas, R. Mishra, Band gap insensitivity to large chemical pressures in ternary bismuth iodides for photovoltaic applications, J. Phys. Chem. C 120 (2016) 28924–28932.

[10] X.G. Zhao, D. Yang, J.C. Ren, Y. Sun, Z. Xiao, L. Zhang, Rational design of halide double perovskites for optoelectronic applications, Joule 2 (2018) 1662–1673.

[11] Z. Xiao, Y. Yan, Progress in theoretical study of metal halide perovskite solar cell materials, Adv. En. Mat. 7 (2017), 1701136.

[12] A.N. Usoltsev, N.A. Korobeynikov, A.S. Novikov, P.E. Plyusnin, B.A. Kolesov, V.P. Fedin, M.N. Sokolov, S.A. Adonin, One-dimensional diiodine-iodobismuthate (III) hybrids Cat₃{[Bi₂I₉](I₂)₃}: syntheses, stability, and optical properties, Inorg. Chem. 59 (2020) 17320–17325.

[13] W. Zhang, X. Liu, L. Li, Z. Sun, S. Han, Z. Wu, J. Luo, Triiodide-induced band-edge reconstruction of a lead-free perovskite-derivative hybrid for strong light absorption, Chem. Mater. 30 (2018) 4081–4088.

[14] J.K. Pious, C. Muthu, S. Dani, A. Saeki, V.C. Nair, Bismuth-based zero-dimensional perovskite-like materials: effect of benzylammonium on dielectric confinement and photoconductivity, Chem. Mat. 32 (2020) 2647–2652.

[15] C. Hrizi, A. Samet, Y. Abid, S. Chaabouni, M. Fliyou, A. Koumina, Crystal structure, vibrational and optical properties of a new self-organized material containing iodide anions of bismuth (III), [C₆H₄(NH₃)₂]₂Bi₂I₁₀·4H₂O, J. Mole. Stru. 992 (2011) 96–101.

[16] P. Hao, W. Wang, J. Shen, Y. Fu, Non-transient thermo-photochromism of iodobismuthate hybrids directed by solvated metal cations, Dalton Trans 49 (2020) 1847–1853.

[17] Y. Zhang, F. Fadaei Tirani, P. Pattison, K. Schenk-Joss, Z. Xiao, M.K. Nazeeruddin, P. Gao, Zero-dimensional hybrid iodobismuthate derivatives: from structure study to photovoltaic application, Dalton Trans 49 (2020) 5815–5822.

[18] C. Katan, N. Mercier, J. Even, Quantum and dielectric confinement effects in lower-dimensional hybrid perovskite semiconductors, Chem. Rev. 119 (2019) 3140–3192.

[19] I.W.H. Oswald, H. Ahn, J.R. Neilson, Influence of organic cation planarity on structural templating in hybrid metal-halides, Dalton Trans 48 (2019) 16340–16349.

[20] G.E. Wang, C. Sun, M.S. Wang, G.C. Guo, Semiconducting crystalline inorganic-organic hybrid metal halide nanochains, Nanoscale 12 (2020) 4771–4789.

[21] L.Y. Han, P. Wang, Q. Wu, Z. Wang, Y.Y. Liu, Z.K. Zheng, H.F. Cheng, Y. Dai, B.B. Huang, Design the π-stacking type of perovskite-like iodobismuthates to enhance their optoelectronic properties, J. Mol. Struct. 1247 (2022), 131332.

[22] G.K.J. Furthmuller, Efficient iterative schemes for ab initio total-energy calculations using a plane-wave basis set, Phys. Rev. B 54 (1996) 11169–11186.

[23] P.E. Blochl, Projector augmented-wave method, Phys. Rev. B 50 (1994) 17953–17979.

[24] G.K.D. Joubert, From ultra soft pseudopotentials to the projector augmented-wave method, Phys. Rev. B 59 (1999) 1758–1775.

[25] John P. Perdew, Kieron Burke, M. Ernzerhof, Generalized gradient approximation made simple, Phys. Rev. Let. 77 (1996) 3865–3868.

[26] Y. Wang, S. Han, Y. Liu, Y. Li, Z. Sun, J. Luo, A lead-free organicnorganic halide perovskite absorber with photoconductive response, Chem. Asian. J. 15 (2020) 3350–3355.

[27] Y.Q. Hu, H.Y. Hui, W.Q. Lin, H.Q. Wen, D.S. Yang, G.D. Feng, Crystal and band-gap engineering of one-dimensional antimony/bismuth-based organic-inorganic hybrids, Inorg. Chem. 58 (2019) 16346–16353.

[28] T. Li, Y. Hu, C.A. Morrison, W. Wu, H. Han, N. Robertson, Lead-free pseudo-three-dimensional organic–inorganic iodobismuthates for photovoltaic applications, Sustain. Energ. Fuels 1 (2017) 308–316.

[29] N.A. Yelovik, A.V. Mironov, M.A. Bykov, A.N. Kuznetsov, A.V. Grigorieva, Z. Wei, E.V. Dikarev, A.V. Shevelkov, Iodobismuthates containing one-dimensional BiI₄ anions as prospective light-harvesting materials: synthesis, crystal and electronic structure, and optical properties, Inorg. Chem. 55 (2016) 4132–4140.

[30] T.A. Shestimerova, N.A. Golubev, N.A. Yelavik, M.A. Bykov, A.V. Grigorieva, Z. Wei, E.V. Dikarev, A.V. Shevelkov, Role of I₂ molecules and weak interactions in supramolecular assembling of pseudo-three-dimensional hybrid bismuth polyiodides: synthesis, structure, and optical properties of phenylenediammonium polyiodobismuthate(III), cryst, Growth Des 18 (2018) 2572–2578.

[31] J. Pal, A. Bhunia, S. Chakraborty, S. Manna, S. Das, A. Dewan, S. Datta, A. Nag, Synthesis and optical properties of colloidal M₃Bi₂I₉ (M = Cs, Rb) perovskite nanocrystals, J. Phys. Chem. C 122 (2018) 10643–10649.

[32] X.L. Li, L.L. Gao, B. Ding, Q.Q. Chu, Z. Li, G.J. Yang, (C₆H₅NH₃)BiI₄: a lead-free perovskite with >330 days humidity stability for optoelectronic applications, J. Mater. Chem. A 7 (2019) 15722–15730.

[33] A.J. Dennington, M.T. Weller, Synthesis and structure of pseudo-three dimensional hybrid iodobismuthate semiconductors, Dalton Trans 45 (2016) 17974–17979.

[34] Z. Xiao, W. Meng, J. Wang, Y. Yan, Thermodynamic stability and defect chemistry of bismuth-based lead-free double perovskites, ChemSusChem 9 (2016) 2628–2633.